2024 American Control Conference (ACC)
July 8-12, 2024. Toronto, Canada

Distributed Neighbor Selection for Second-order Semi-Autonomous Networks

Jingbo Yang, Haoyu Wei, Lulu Pan, *Member, IEEE,* Haibin Shao, *Member, IEEE,* Dewei Li and Yang Lu

***Abstract*—This paper examines the distributed neighbor selection problem for second-order semi-autonomous multi-agent networks. By inheriting the leader-to-follower reachability property encoded in the eigenvector associated with the smallest eigenvalue of perturbed graph Laplacian, this paper shows that the convergence rate of a second-order semi-autonomous network can be enhanced on the reduced network constructed by this eigenvector. Moreover, a quantitative connection between the relative rate of change in velocity of neighboring agents and the corresponding entries in this eigenvector is also established, enabling a distributed neighbor selection algorithm for second-order multi-agent networks. The main results in this paper extend our previous work of distributed neighbor selection algorithm design to multi-agent networks with more complicated agent-level dynamics.**

***Index Terms*—Semi-autonomous network, leader-to-follower reachability, distributed neighbor selection, second-order system, Laplacian eigenvector.**

I. Introduction

Reaching consensus via local information exchange is an essential routine for distributed algorithms implemented on multi-agent networks [1], [2], [3], [4], [5]. Here, a notable fact is that the convergence rate of the consensus process dramatically signifies the performance of consensus-based distributed algorithms [6], [7]. It is well-known that the connectivity of the underlying communication networks, realized via each agent's interactions with its nearest neighbors, plays a central role in the convergence rate of multi-agent networks [8], [9], [10], [11]. However, the convergence rate may vary considerably among all possible connected network configurations [2], [9], [10], [11], [12], [13].

Recall that the consensus problem originates in the swarming phenomenon of natural species, such as a flock of birds and a school of fishes [8], [14]. It would be illuminating to note that, for instance, in flocks of starlings, each bird interacts only with six to seven nearest neighbors rather than with all birds within a sensing radius [15]. The relevant observations motivate the development of distributed neighbor selection algorithms for first-order multi-agent networks [16], [17], which is a convenient paradigm for convergence rate enhancement via local edge reduction. Recently, an eigenvector-based distributed neighbor selection algorithm has been developed to enhance the convergence rate of multi-agent networks [16], [17], [18]. The analytical procedures in this line of work typically deal with three issues:

First, construct a reduced network that guarantees the leader-to-follower reachability via a specific eigenvector of perturbed graph Laplacian;

Second, analyze the enhancement of the convergence rate on this reduced network;

Finally, explore local measurable information amongst agents for distributed construction of this reduced network.

However, the existing results only consider multi-agent systems with first-order local dynamics [16], [17]. For multi-agent networks with specific dynamics, the relevant results are still lacking, hindering the applicability of the proposed distributed neighbor selection framework.

This paper is intended to extend previous results in [16] by examining the distributed neighbor selection problem of second-order semi-autonomous multi-agent networks. The main contributions of this paper are summarized as follows. By inheriting the leader-to-follower reachability encoded in the eigenvector associated with the smallest eigenvalue of the perturbed graph Laplacian, we show that the convergence rate of second-order semi-autonomous networks can be enhanced on the reduced network constructed by this eigenvector. Moreover, a quantitative connection between the states of neighboring agents and the entries of this eigenvector is also established, enabling the distributed implementation of the construction of the reduced network, which shall be referred to as distributed neighbor selection in our discussion. The main results in this paper extend our previous work to multi-agent networks with more complicated agent dynamics, promoting the application of our theoretical findings to real-world multi-agent networks.

The remainder of this paper is organized as follows. The second-order semi-autonomous multi-agent network is introduced in §2. Then, we formulate the problem and introduce the construction of the reduced network via the eigenvector of the perturbed graph Laplacian in §3. The convergence rate enhancement of the second-order semi-autonomous multi-agent system on the reduced network is analyzed in §4, which is followed by the distributed neighbor selection algorithm for second-order semi-autonomous multi-agent networks presented in §5. The concluding remarks are provided in §6.

II. Second-order Multi-agent Network

Consider a second-order semi-autonomous multi-agent network with $n \in \mathbb{N}$ agents, denoted by an undirected $\mathcal{G} =$

This work was supported by the National Science Foundation of China (Grant No. 62103278, 62373244, 61973214, 61963030).

The Jingbo Yang, Haoyu Wei, Lulu Pan, Haibin Shao, and Dewei Li are with the Department of Automation, Shanghai Jiao Tong University, Shanghai, 200240, China.

The Yang Lu is with the school of Computing and Communications, Lancaster University, Lancaster, LA1 4WA, United Kingdom.

979-8-3503-8265-5/$31.00 ©2024 AACC

$(\mathcal{V}, \mathcal{E}, W)$, edge set $\mathcal{E} \subseteq \mathcal{V} \times \mathcal{V}$ and adjacency matrix $W = [w_{ij}] \in \mathbb{R}^{n\times n}$ satisfying $w_{ij} = 1$ if $(j,i) \in \mathcal{E}$ and $w_{ij} = 0$ otherwise. Each agent $i \in \mathcal{V}$ in $\mathcal{G}$ possesses a positional state $\boldsymbol{x}_i(t) \in \mathbb{R}^d$ and a state of velocity $\boldsymbol{v}_i(t) \in \mathbb{R}^d$ within a d-dimensional space where $d \in \mathbb{N}$ [19]. The neighbor set of agent i is denoted by $\mathcal{N}_i = \{j \in \mathcal{V} \,|\, (j,i) \in \mathcal{E}\}$. The Laplacian of $\mathcal{G}$ is denoted by $L = [l_{ij}] \in \mathbb{R}^{n\times n}$, whose entries satisfying that $l_{ij} = \sum_{j=1}^{n} w_{ij}$ for $i = j$ and $-w_{ij}$ for $i \neq j$.

In a semi-autonomous network $\mathcal{G}$, $m \in \mathbb{N}\,(m < n)$ agents are designated as leader agents, leaving $n - m$ agents as followers. Leader agents are in charge of receiving external inputs to steer the network towards a desired state. The dynamics of each agent i is governed by

$$\begin{cases} \dot{\boldsymbol{x}}_i(t) = \boldsymbol{v}_i(t) \\ \dot{\boldsymbol{v}}_i(t) = \boldsymbol{u}_i(t) \end{cases} \tag{1}$$

where $\boldsymbol{x}_i(t) \in \mathbb{R}^d$, $\boldsymbol{v}_i(t) \in \mathbb{R}^d$, and $\boldsymbol{u}_i(t) \in \mathbb{R}^d$ for $i \in \mathcal{V}$ represent the position, longitudinal velocity and control input of agent i at time t, respectively. Each leader agent is subject to the influence of an external input with a constant velocity whose dynamics are therefore dictated by

$$\begin{cases} \dot{\boldsymbol{x}}_j^E(t) = \boldsymbol{v}_0 \\ \dot{\boldsymbol{v}}_j^E(t) = \boldsymbol{0} \end{cases} \tag{2}$$

where $\boldsymbol{x}_j^E(t) \in \mathbb{R}^d$ and $\boldsymbol{v}_j^E(t) \in \mathbb{R}^d\,(j = \underline{m})$ represent the homogeneous position and velocity of the external inputs, respectively, with $\boldsymbol{x}_j^E(0) = 0$. Moreover, we let $\boldsymbol{v}_j^E(t) = \boldsymbol{v}_0$ represent a constant input in velocity that drives the evolution of the entire network. The input matrix $B = [b_{il}] \in \mathbb{R}^{n\times m}$ is defined such that $b_{il} = 1$ if and only if agent i is a leader, and $b_{il} = 0$ otherwise.

Consider the following diffusive interaction protocol

$$\begin{aligned} \boldsymbol{u}_i(t) = & -\alpha \sum_{j=1}^{n} w_{ij}\left(\boldsymbol{x}_i(t) - \boldsymbol{x}_j(t)\right) \\ & - \beta \sum_{j=1}^{n} w_{ij}\left(\boldsymbol{v}_i(t) - \boldsymbol{v}_j(t)\right) \\ & - b_{il}\left[\alpha\left(\boldsymbol{x}_i(t) - \boldsymbol{x}_l^E(t)\right) + \beta\left(\boldsymbol{v}_i(t) - \boldsymbol{v}_0\right)\right],\ i \in \mathcal{V}, \end{aligned} \tag{3}$$

where the coupling strength coefficients $\alpha > 0$ and $\beta > 0$ are the same for all agents. The overall dynamics of the second-order multi-agent network under protocol (3) can be characterized by

$$\begin{bmatrix} \dot{\boldsymbol{x}}(t) \\ \dot{\boldsymbol{v}}(t) \end{bmatrix} = (H_1 \otimes I_d)\begin{bmatrix} \boldsymbol{x}(t) \\ \boldsymbol{v}(t) \end{bmatrix} + (H_2 \otimes I_d)\begin{bmatrix} \boldsymbol{x}^E(t) \\ \boldsymbol{v}^E(t) \end{bmatrix}, \tag{4}$$

where $\boldsymbol{x}(t) = \left(\boldsymbol{x}_1^\top(t), \ldots, \boldsymbol{x}_n^\top(t)\right)^\top$, $\boldsymbol{v}(t) = \left(\boldsymbol{v}_1^\top(t), \ldots, \boldsymbol{v}_n^\top(t)\right)^\top$, $\boldsymbol{x}^E(t) = \left(\boldsymbol{x}_1^{E^\top}(t), \ldots, \boldsymbol{x}_m^{E^\top}(t)\right)^\top$, $\boldsymbol{v}^E(t) = \left(\boldsymbol{v}_0^\top, \ldots, \boldsymbol{v}_0^\top\right)^\top \in \mathbb{R}^{md}$, and

$$H_1 = \begin{bmatrix} \boldsymbol{0}_{n\times n} & I_n \\ -\alpha L_B & -\beta L_B \end{bmatrix},\ H_2 = \begin{bmatrix} \boldsymbol{0}_{n\times m} & \boldsymbol{0}_{n\times m} \\ \alpha B & \beta B \end{bmatrix},$$

where I_d is the $d \times d$ identity matrix, $\boldsymbol{1}_m$ and $\boldsymbol{0}_{n\times m}$ denote $m \times 1$ vector and $n \times m$ matrix of all ones and all zeros, respectively, and

$$L_B = L + \mathbf{diag}(B\boldsymbol{1}_m), \tag{5}$$

where L_B is referred to as perturbed Laplacian matrix [17].

The second-order semi-autonomous networks (second-order SANs) under protocol (3) is said to achieve the *leader-follower consensus* if $\lim_{t\to+\infty} ||\boldsymbol{v}_i(t) - \boldsymbol{v}_0|| = 0$ and $\lim_{t\to+\infty} ||\boldsymbol{x}_i(t) - \boldsymbol{x}_j^E(t)|| = 0$ for all $i \in \mathcal{V},\ j \in \underline{m}$ and some norm on $\mathbb{R}^d$ [20]. The Euclidean norm of a vector $\boldsymbol{x} \in \mathbb{R}^{n\times n}$ is designated by $||\boldsymbol{x}|| = (\boldsymbol{x}^\top \boldsymbol{x})^{\frac{1}{2}}$.

We first introduce the following lemma provided in [21] for the consensus in second-order fully-autonomous networks (second-order FANs), alternatively, the consensus in second-order multi-agent networks without leaders. The overall dynamics of second-order FANs can be characterized by

$$\begin{bmatrix} \dot{\boldsymbol{x}}(t) \\ \dot{\boldsymbol{v}}(t) \end{bmatrix} = (H_0 \otimes I_d)\begin{bmatrix} \boldsymbol{x}(t) \\ \boldsymbol{v}(t) \end{bmatrix}, \tag{6}$$

where

$$H_0 = \begin{bmatrix} \boldsymbol{0}_{n\times n} & I_n \\ -\alpha L & -\beta L \end{bmatrix} \in \mathbb{R}^{2n\times 2n}.$$

Lemma 1. *[21] Second-order FANs* (6) *can achieve consensus if and only if matrix H_0 has exactly one zero eigenvalue of multiplicity of two and all the other eigenvalues have real parts. Moreover, if second-order consensus is reached, $\lim_{t\to+\infty} ||\boldsymbol{v}_i(t) - \sum_{j=1}^{n} \boldsymbol{\xi}_j \boldsymbol{v}_j(0)|| = 0$ and $\lim_{t\to+\infty} ||\boldsymbol{x}_i(t) - \sum_{j=1}^{n} \boldsymbol{\xi}_j \boldsymbol{x}_j(0) - \sum_{j=1}^{n} \boldsymbol{\xi}_j \boldsymbol{v}_j(0)t|| = 0$, where $\boldsymbol{\xi}$ is the unique nonnegative left eigenvector of L with eigenvalue 0 satisfying $\boldsymbol{\xi}^\top \boldsymbol{1}_n = 1$.*

Inspired by the proof of Lemma 1, if all the eigenvalues of H_1 possess negative real parts, the states of agents will converge to the linear combination of the states of external inputs. Let ς_{ij} denote the eigenvalues of H_1 where $i \in \underline{n}$ and $j \in \underline{2}$. We can order the eigenvalues of the perturbed Laplacian matrix L_B as $0 < \lambda_1 \leq \lambda_2 \leq \ldots \leq \lambda_n$ with corresponding normalized eigenvectors $\boldsymbol{\phi}_1, \boldsymbol{\phi}_2, \ldots, \boldsymbol{\phi}_n$. Moreover, λ_1 is a simple eigenvalue and $\boldsymbol{\phi}_1$ can be chosen to be positive [17]. Then eigenvalues of H_1 can be written as,

$$\varsigma_{i1} = \frac{-\beta\lambda_i + \sqrt{\beta^2\lambda_i^2 - 4\alpha\lambda_i}}{2},$$

and

$$\varsigma_{i2} = \frac{-\beta\lambda_i - \sqrt{\beta^2\lambda_i^2 - 4\alpha\lambda_i}}{2}. \tag{7}$$

Note that all the eigenvalues of H_1 have negative real parts if $\alpha, \beta > 0$, implying that the second-order SAN (4) can achieve leader-follower consensus.

III. Eigenvector-based Reduced Network

In this paper, we shall examine distributed neighbor selection algorithm design for second-order SANs. Following the paradigm of our previous work [17], the designed distributed neighbor selection algorithm needs to guarantee that one can

1) construct a reduced network from a second-order SAN via perturbed Laplacian eigenvector,

2) analyze the enhancement of convergence rate on the reduced network and

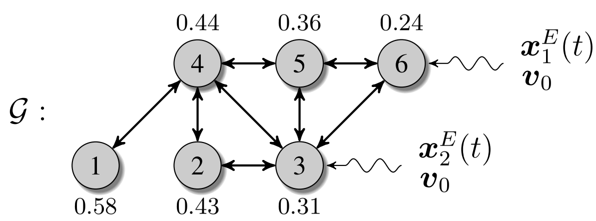

Figure 1. Original network. Node 3 and node 6 are agents influenced by external inputs $x_j^E(t)\,(j=1,2)$ and v_0.

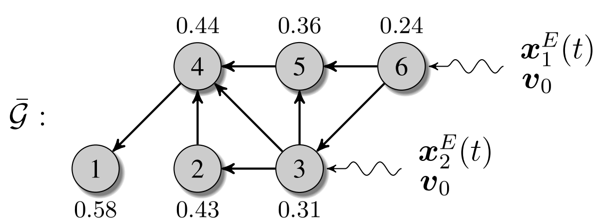

Figure 2. $\bar{\mathcal{G}}$: The FSN network of $\mathcal{G}$ in Figure 1.

3) employ proper local measurable information for distributed implementation of neighbor selection.

The construction of the reduced network using the eigenvector associated with the smallest eigenvalue of the perturbed Laplacian matrix has been shown to be valid in convergence rate enhancement of first-order SANs in [16], [17]. Thus, the main concentration of this paper is to examine the convergence rate enhancement on the reduced network for second-order SANs (Theorem 1) and investigate how to relate the locally observable information to the eigenvector for the distributed implementation of the neighbor selection (Theorem 2).

To see the construction of the reduced network using the eigenvector associated with the smallest eigenvalue of L_B, we first provide an example for illustration. A subgraph $\bar{\mathcal{G}} = (\bar{\mathcal{V}}, \bar{\mathcal{E}}, \bar{W})$ of a graph $\mathcal{G}$ is a graph such that $\bar{\mathcal{V}} \subset \mathcal{V}$ and $\bar{\mathcal{E}} \subset \mathcal{E}$.

Example 1. Consider an undirected 6-nodes multi-agent network $\mathcal{G}$ in Figure 1. Agent 3 and 6 are leader agents influenced by homogenous inputs $\boldsymbol{x}_l^E(t) \in \mathbb{R}^3$, $l = 1, 2$ and $\boldsymbol{v}_0$. Then, the eigenvector $\boldsymbol{\phi}_1(L_B)$ associated with the smallest eigenvalue $\lambda_1(L_B) = 0.2332$ of perturbed Laplacian L_B is,

$$\boldsymbol{\phi}_1(L_B) = (0.58, 0.43, 0.31, 0.44, 0.36, 0.24)^\top .$$

Here, $\bar{\mathcal{G}}$ is the reduced network that will be formally defined in Definition 1 as depicted in Figure 2. A path $\mathcal{P}$ in a network $\mathcal{G}$ is a concatenation of edges denoted by $\mathcal{P} = \{(i_1, i_2), (i_2, i_3), \ldots, (i_{p-1}, i_p)\} \subset \mathcal{E}$, where all nodes $i_1, i_2, \ldots, i_p \in \mathcal{V}$ are distinct. A node i is reachable from $j \in \mathcal{V}$ if there exists a directed path from j to i. One can observe that for each agent $i \in \mathcal{V}$, there exists a directed path from one of the external inputs to agent i and the entries in $\boldsymbol{\phi}_1(L_B)$ along the path exhibit a monotonically increasing trend. Consequently, the reduced network can exhibit consensus depending on the leader-to-follower reachability.

We shall first recall some facts on the smallest eigenvalue of perturbed Laplacian and its associated eigenvector.

Lemma 2. *[22] Let $\lambda_1(L_B)$ and $\boldsymbol{\phi}_1(L_B)$ denote the smallest eigenvalue and the corresponding normalized eigenvector of L_B, respectively. Then $\lambda_1(L_B) > 0$ is a simple eigenvalue of L_B and $\boldsymbol{\phi}_1(L_B)$ can be chosen to be a positive vector.*

By following the terminology in [17], the reduced network $\bar{\mathcal{G}}$ in Example 1 is called FSN (follow the slower neighbor) network. The FSN networks are a class of reduced networks for second-order SANs generated by eliminating a subset of edges using information encoded in $\boldsymbol{\phi}_1(L_B)$ [17]. This elimination procedure is referred to as neighbor selection. Following this process, each agent tracks its neighbors who exhibit a relatively slower rate of change in velocity. The following is the definition of the FSN networks in which information encoded in $\boldsymbol{\phi}_1(L_B)$ is applied for neighbor selection. The entry located at the ith row and jth column in a matrix $M \in \mathbb{R}^{n\times n}$ is denoted by $[M]_{ij}$ and the ith entry of a vector $\boldsymbol{x}$ by $[\boldsymbol{x}]_i$. Notably, $\frac{[x]_i}{[x]_j}$ is denoted by x_{ij}.

Definition 1 (Reduced Network)**.** [22] Let $\mathcal{G} = (\mathcal{V}, \mathcal{E}, W)$ be a second-order SAN with the input matrix B. The FSN network of $\mathcal{G}$, denoted by $\bar{\mathcal{G}} = (\bar{\mathcal{V}}, \bar{\mathcal{E}}, \bar{W})$, is a subgraph of $\mathcal{G}$ such that $\bar{\mathcal{V}} = \mathcal{V}, \bar{\mathcal{E}} \subseteq \mathcal{E}$ and $\bar{W} = (\bar{w}_{ij}) \in \mathbb{R}^{n\times n}$, where $\bar{w}_{ij} = w_{ij}$ if $\boldsymbol{\phi}_1(L_B)_{ij} > 1$ and $\bar{w}_{ij} = 0$ when $\boldsymbol{\phi}_1(L_B)_{ij} \leq 1$.

Note that the leader-to-follower reachability of the FSN network can be guaranteed, which has been proven in [17]. Alternatively, after removing specific edges from the original network $\mathcal{G}$ according to Definition 1, there remains accessibility from external inputs to all agents in the FSN network.

IV. Convergence Rate Enhancement on Reduced Network

The enhancement of convergence rate on first-order SANs prompts us to inquire whether the neighbor selection approach continues to exhibit favorable performance when the dynamics of agents admit the second-order dynamics [17]. In this section, we proceed to examine the convergence rate enhancement of second-order SANs on the reduced networks, i.e., FSN network. Different from the first-order SANs, although the convergence rate of multi-agent network (4) is determined by the parameters (α and β) and the network topology, we can still assert that, in the FSN network, the convergence rate consistently outperforms that in the original network.

We shall first provide an example to illustrate the convergence rate enhancement before the formal analysis.

Example 2. We set homogenous input $\boldsymbol{x}_j^E(t) = (0.7, 0.8, 0.9)^\top$, $\dot{\boldsymbol{x}}_j^E(t) = \boldsymbol{v}_0$ $(j = 1, 2)$ and $\boldsymbol{v}_0 = (1, 2, 4)^\top$ in Example 1, representing that the velocities of agents in the network will be driven towards $\boldsymbol{v}_0$ under the influence of agent 3 and 6. The agents' positions are randomly selected from $[0, 100] \times [0, 100] \times [0, 100]$, and the initial velocities of agents are zeros. The strength coefficients are $\alpha = \beta = 1$. Figure 3 illustrates the convergence rate comparison of the velocities of agents in the original network $\mathcal{G}$ and FSN

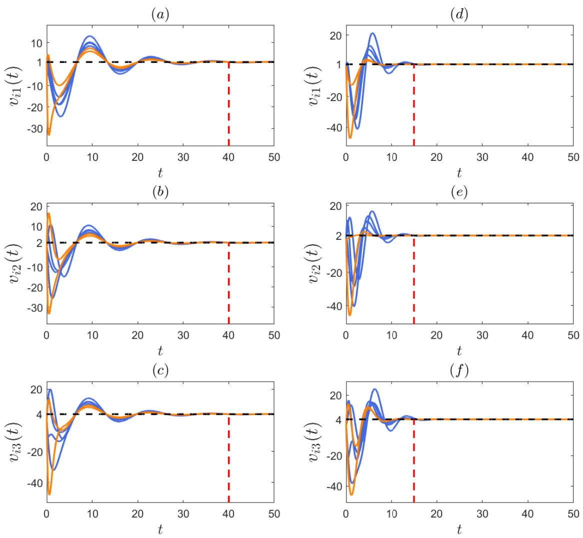

Figure 3. Velocity trajectories of agents in the second-order SAN in Figure 1 (left side (a)-(c)) and in the FSN network in Figure 2 (right side (d)-(f)). The black dotted line in each panel represents the external input of velocity. The blue lines represent the trajectories of followers, while the orange lines represent leaders. The red dotted line represents the time of convergence.

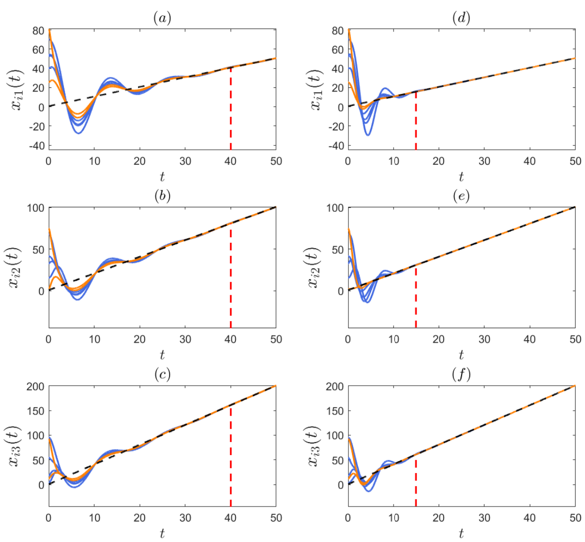

Figure 4. Position trajectories of agents in the second-order SAN in Figure 1 (left side (a)-(c)) and in the FSN network in Figure 2 (right side (d)-(f)). The black dotted line in each panel represents the exteral input of position. The blue lines represent the trajectories of followers, while the orange lines represent leaders. The red dotted line represents the time of convergence.

network $\bar{\mathcal{G}}$, while Figure 4 illustrates the convergence rate comparison of the positions of agents.

The convergence rates of both velocity and position are significantly enhanced in the FSN network compared to the original network, demonstrating that the neighbor selection approach in Definition 1 remains effective for second-order SANs.

Next, we will show that convergence rate enhancement on the FSN network compared with the original second-order SAN holds across various combinations of strength coefficients and network topology.

The theoretical guarantee of convergence rate enhancement for first-order SANs is provided in [17]. Previous research on second-order SANs (4) indicates that the system's convergence rate is intricately influenced by the combination of α, β, along with the smallest or largest non-zero eigenvalues of the perturbed Laplacian L_B (represented as λ_1 and λ_n, respectively). Specifically, with fixed strength coefficients α, β, the exponential convergence rate of second-order SANs can be determined by the real parts of specific the eigenvalues of matrix H_1 [23],

$$c(\lambda_1, \lambda_n) = \min \{c_1(\lambda_1), c_2(\lambda_n)\}, \tag{8}$$

where

$$\begin{aligned} c_1(\lambda_1) &= \frac{\beta\lambda_1}{2}, \\ c_2(\lambda_n) &= \frac{\beta\lambda_n - \sqrt{\beta^2\lambda_n^2 - 4\alpha\lambda_n}}{2} \\ &= \frac{2\alpha}{\beta + \sqrt{\beta^2 - 4\alpha\frac{1}{\lambda_n}}}. \end{aligned}$$

We present the following theorem to show that the FSN network generated from a second-order SAN will also enhance the convergence rate of (4).

Theorem 1. *Let $\bar{\mathcal{G}} = (\mathcal{V}, \bar{\mathcal{E}}, \bar{W})$ denote the FSN network of a second-order SAN $\mathcal{G} = (\mathcal{V}, \mathcal{E}, W)$ with the input matrix B. Then,*

$$\lambda_1(L_B(\bar{\mathcal{G}})) \geq \lambda_1(L_B(\mathcal{G})), \tag{9}$$

where equality holds only when all agents are leaders and

$$\lambda_n(L_B(\bar{\mathcal{G}})) \leq \lambda_n(L_B(\mathcal{G})), \tag{10}$$

where the inequality is strict when there exist no agent that is connected to all other agents.

Remark 1. This theorem provides a theoretical guarantee of convergence rate enhancement on FSN networks compared with the original network. The equality in Theorem 1 holds only in irregular cases. Specifically, equality holds for (9) when all agents are leaders. As for (10), equality will not hold when no agent is connected to all other agents, which is a common scenario since it is often assumed that each agent in the network is only connected to a subset of agents for distributed implementation.

Note that $c_1(\lambda_1)$ is a monotonically increasing function with respect to λ_1, and $c_2(\lambda_n)$ is a monotonically decreasing function with respect to λ_n. Denote the smallest (largest) eigenvalue of $L_B(\mathcal{G})$ and $L_B(\bar{\mathcal{G}})$ as λ_1 (λ_n) and $\lambda_1^{'}$ ($\lambda_n^{'}$), respectively. By applying Theorem 1, and excluding the aforementioned irregular cases, one has that $c_1\left(\lambda_1^{'}\right) > c_1\left(\lambda_1\right)$ and $c_2\left(\lambda_n^{'}\right) > c_2\left(\lambda_n\right)$. Therefore,

$$\begin{aligned} c\left(\lambda_1^{'}, \lambda_n^{'}\right) &= \min\left\{c_1(\lambda_1^{'}), c_2(\lambda_n^{'})\right\} \\ &> \min\left\{c_1(\lambda_1), c_2(\lambda_n)\right\} \\ &= c\left(\lambda_1, \lambda_n\right). \end{aligned}$$

This implies that if the irregular cases in Remark 1 are excluded, the FSN network always converges faster than that on the original network, regardless of the strength coefficients and the topology of the original network. Notably, the convergence rate on the FSN network is never slower than that on the original network, even in those irregular cases.

V. Neighbor Selection via Local Information

In this section, we shall show how to employ the relative tempo of velocity of second-order consensus networks for distributed neighbor selection algorithm design. In essence, protocol (3) employs the deviation of neighboring agents in a multi-agent network to construct a local feedback control rule that achieves an aggregation of the states of all agents from a global perspective [10]. Here, we use a ratio-form quantity to capture the velocity deviation of neighboring agents and show how the proposed quantity can distinguish agents in a consensus network and subsequently enhance the convergence performance.

Without loss of generality, let us regard the homogenous external inputs as one input $\boldsymbol{u} = \left(\boldsymbol{u}_x^\top, \boldsymbol{u}_v^\top\right)^\top = \left(\int_0^t \boldsymbol{v}_0^\top dt, \boldsymbol{v}_0^\top\right)^\top$. Denote $\boldsymbol{\chi}(t) = \left(\boldsymbol{x}^\top(t), \boldsymbol{v}^\top(t), \boldsymbol{u}_x^\top, \boldsymbol{u}_v^\top\right)^\top$. Then the overall dynamics (4) can be rewritten as

$$\dot{\boldsymbol{\chi}}(t) = M\boldsymbol{\chi}(t) \tag{11}$$

where matrix M is defined as

$$M = \begin{bmatrix} \mathbf{0}_{n\times n} & I_n & \mathbf{0}_{n\times 1} & \mathbf{0}_{n\times 1} \\ -\alpha L_B & -\beta L_B & \alpha B\mathbf{1}_m & \beta B\mathbf{1}_m \\ \mathbf{0}_{1\times n} & \mathbf{0}_{1\times n} & 0 & 1 \\ \mathbf{0}_{1\times n} & \mathbf{0}_{1\times n} & 0 & 0 \end{bmatrix}.$$

To focus on the velocity of each agent, we introduce the selection matrix. Let $\eta = \{i_1, i_2, ..., i_l\}$. For a set of agents $\Phi = \{v_{i_1}, v_{i_2}, \dots, v_{i_l}\} \subset \mathcal{V}$, the corresponding selection matrix $h(\Phi)$ is referred to as

$$h(\Phi) = h(\eta) = \begin{bmatrix} \mathbf{0}_{1\times n} & \boldsymbol{e}_{i_1} & \mathbf{0}_{1\times 2} \\ \mathbf{0}_{1\times n} & \boldsymbol{e}_{i_2} & \mathbf{0}_{1\times 2} \\ \mathbf{0}_{1\times n} & \vdots & \mathbf{0}_{1\times 2} \\ \mathbf{0}_{1\times n} & \boldsymbol{e}_{i_l} & \mathbf{0}_{1\times 2} \end{bmatrix} \otimes I_d,$$

where $\boldsymbol{e}_{i_l}$ represents the i_l-th row of the identity matrix I_n. To distinguish different set of agents, we have defined that $\eta_k = \{i_1, i_2, ..., i_l\}$, $h_k = h(\eta_k),\ k \in \mathbb{N}$ and $\Theta_k = \Theta(\eta_k) = \begin{bmatrix} \boldsymbol{e}_{i_1}^\top, & \boldsymbol{e}_{i_2}^\top, & \dots, & \boldsymbol{e}_{i_l}^\top \end{bmatrix}^\top$ for set $\mathcal{V}_k$.

Here, we are primarily concerned with the relative tempo of the agents' velocities $\boldsymbol{v}_i(t) \in \mathbb{R}^d$ (will be formally defined in Definition 2). Therefore, the state vector of agents' velocities in Φ selected by $h(\Phi)$ can thus be represented by

$$h(\Phi)\boldsymbol{\chi}(t) = \begin{pmatrix} \boldsymbol{v}_{i_1}^\top(t), & \boldsymbol{v}_{i_2}^\top(t), & \dots & \boldsymbol{v}_{i_l}^\top(t) \end{pmatrix}^\top.$$

In the sequel, we present the definition of relative tempo of velocity for second-order SANs, and show that the relative tempo of velocity is quantitively associated with $\boldsymbol{\phi}_1(L_B)$, which allows utilizing local information to implement the neighbor selection algorithm.

Definition 2 (Relative Tempo of Velocity)**.** Let $\mathcal{V}_1 \subset \mathcal{V}$ and $\mathcal{V}_2 \subset \mathcal{V}$ be two subgroups of agents in multi-agent network (11), and $h(\mathcal{V}_1)$ and $h(\mathcal{V}_2)$ are selection matrices of $\mathcal{V}_1$ and $\mathcal{V}_2$, respectively. Then the *relative tempo of velocity* between agents in $\mathcal{V}_1$ and $\mathcal{V}_2$ is

$$\mathbf{RT}(\mathcal{V}_1, \mathcal{V}_2) = \lim_{t\to\infty} \frac{\|h(\mathcal{V}_1)\dot{\boldsymbol{\chi}}(t)\|}{\|h(\mathcal{V}_2)\dot{\boldsymbol{\chi}}(t)\|}. \tag{12}$$

We now provide a sufficient condition under which the convergence rate of the original second-order SAN (11) is uniquely determined by the smallest eigenvalue of perturbed Laplacian L_B, to support the subsequent proof.

Lemma 3. *If the strength coefficients α, β in second-order SANs* (11) *satisfy that $\frac{\alpha}{\beta^2} \geq \frac{1}{2}$, the convergence rate of second-order SANs is determined by the smallest eigenvalue of the perturbed Laplacian L_B.*

Similar to the result for the first-order SANs, the relative tempo of velocity in second-order SANs (11) is still encoded in $\boldsymbol{\phi}_1(L_B)$, but in a more complicated manner.

Theorem 2. *Let $\mathcal{V}_1 \subset \mathcal{V}$ and $\mathcal{V}_2 \subset \mathcal{V}$ be two subgroups of agents in the second-order SAN* (11)*. Let h_1 and h_2 be the selection matrices of $\mathcal{V}_1$ and $\mathcal{V}_2$, respectively. Denote the ordered eigenvalues of L_B as $0 < \lambda_1 < \lambda_2 \leq \cdots \leq \lambda_n$ with corresponding normalized eigenvectors $\boldsymbol{\phi}_1, \boldsymbol{\phi}_2, \dots, \boldsymbol{\phi}_n$. When the strength coefficients α, β satisfy Lemma 3, the relative tempo of velocity between agents in $\mathcal{V}_1$ and $\mathcal{V}_2$ satisfies*

$$\mathbf{RT}(\mathcal{V}_1, \mathcal{V}_2) = \frac{\|\Theta_1\boldsymbol{\phi}_1(L_B)\|}{\|\Theta_2\boldsymbol{\phi}_1(L_B)\|}.$$

Remark 2. The relative tempo of velocity forms a quantitative link in second-order SANs. Specifically, the ratio of the rate of change of velocities between neighboring agents will converge to the ratio corresponding to the eigenvector $\boldsymbol{\phi}_1(L_B)$, and this convergence of ratio occurs significantly earlier than the convergence of the states of position and velocity.

We now provide an example to illustrate the quantitative link provided in Theorem 2.

Example 3. Consider the following quantity of velocity

$$g_{ij} = \frac{||\boldsymbol{v}_i(t)||}{||\boldsymbol{v}_j(t)||},\ i \in \mathcal{V},\ j \in \mathcal{N}_i, \tag{13}$$

which satisfies $\lim_{t\to\infty} g_{ij}(t) = \mathbf{RT}(i, j)$. We now examine the quantitative link of relative tempo and $\boldsymbol{\phi}_1(L_B)$ in Example 2. The trajectories of $g_{ij}(t)$ for $i = 5$ and $j \in \{3, 4, 6\}$ are shown in Figure 5. The steady states of $gij(t)$ are archived at $t = 10$, when $g_{53}(10) = 1.1627$, $g_{54}(10) = 0.8079$ and $g_{56}(10) = 1.4969$. Meanwhile, one has $\boldsymbol{\phi}_1(L_B)_{53} = 1.1643$, $\boldsymbol{\phi}_1(L_B)_{54} = 0.8089$ and $\boldsymbol{\phi}_1(L_B)_{56} = 1.4884$.

Examining the convergence rate of velocities in the original network shown in Figure 3 and that of $g_{ij}(t)$ in Figure 5,

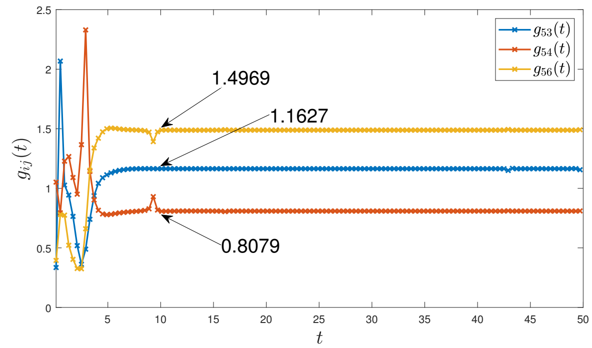

Figure 5. Trajectories of $g_{ij}(t)$ for agent $i = 3$ and its neighbors $j \in \{4, 5, 6\}$ in second-order SAN shown in Example 2.

one observes that the second-order SAN achieves an "ordered" state characterized by the relative tempo of velocity, prior to the final consensus time.

Up to this point, we have demonstrated that in second-order SANs (11), if the strength coefficients satisfy the condition in Lemma 3, the derivative of the agents' velocities will comply with a relationship with $\phi_{\mathbf{1}}(L_B)$. This quantitative link has enabled us to develop a distributed algorithm that leverages local information, instead of global information of a second-order SAN, for neighbor selection to optimize the information flow in the interaction network, thereby enhancing convergence performance.

In the spirit of the relative tempo of velocity, it is instinctive to examine the evolution of a consensus network when agents choose to be directly influenced only by a certain group of neighbors. We shall subsequently introduce the formal definition for the "Follow the Slower Neighbor" network via relative tempo in (12) as follows.

Definition 3 (FSN Network)**.** Let $\bar{\mathcal{G}} = (\mathcal{V}, \bar{\mathcal{E}}, \bar{W})$ denote the FSN network of the second-order SANs (4). Then the FSN network $\bar{\mathcal{G}}$ satisfies that $\bar{w} = [\bar{w}_{ij}] \in \mathbb{R}^{n \times n}$ where $\bar{w}_{ij} = w_{ij}$ if $\mathbf{RT}(\{i\}, \{j\}) \geq 1$ and $\bar{w}_{ij} = 0$ if $\mathbf{RT}(\{i\}, \{j\}) < 1$.

In an FSN network, each agent i always follows those neighbors whose rates of change in velocities are slower than i. Therefore, according to the relative tempo theorem, the tempo network for a second-order SAN can actually be constructed by each agent in a distributed and data-driven fashion without global topology.

VI. Conclusion

This paper addresses the distributed neighbor selection problem for second-order SANs. In this direction, we have applied the relative tempo theory to enhance the convergence rate of second-order SANs. A detailed analysis has been performed to explore the quantitative connection between the entries of the perturbed Laplacian eigenvector and the relative rate of change in velocity (relative tempo of velocity) of agents with second-order dynamics. Moreover, a sufficient condition has been derived to ensure this elegant quantitative connection, and along the way, a data-driven distributed neighbor selection algorithm has been proposed using the relative tempo of velocity between each agent and its neighbors, and theoretical guarantees of convergence rate enhancement of second-order SANs on the corresponding FSN networks have been established.

References

[1] Soon-Jo Chung, Aditya Avinash Paranjape, Philip Dames, Shaojie Shen, and Vijay Kumar. A survey on aerial swarm robotics. *IEEE Transactions on Robotics*, 34(4):837–855, 2018.

[2] Mehran Mesbahi and Magnus Egerstedt. *Graph Theoretic Methods in Multiagent Networks*. Princeton University Press, 2010.

[3] Angelia Nedic. Distributed gradient methods for convex machine learning problems in networks: Distributed optimization. *IEEE Signal Processing Magazine*, 37(3):92–101, 2020.

[4] Anton V Proskurnikov and Roberto Tempo. A tutorial on modeling and analysis of dynamic social networks. part i. *Annual Reviews in Control*, 43:65–79, 2017.

[5] Solmaz S Kia, Bryan Van Scoy, Jorge Cortes, Randy A Freeman, Kevin M Lynch, and Sonia Martinez. Tutorial on dynamic average consensus: The problem, its applications, and the algorithms. *IEEE Control Systems Magazine*, 39(3):40–72, 2019.

[6] Angelia Nedich et al. Convergence rate of distributed averaging dynamics and optimization in networks. *Foundations and Trends® in Systems and Control*, 2(1):1–100, 2015.

[7] Alex Olshevsky and John N Tsitsiklis. Convergence speed in distributed consensus and averaging. *SIAM Journal on Control and Optimization*, 48(1):33–55, 2009.

[8] A. Jadbabaie, Jie Lin, and A.S. Morse. Coordination of groups of mobile autonomous agents using nearest neighbor rules. *IEEE Transactions on Automatic Control*, 48(6):988–1001, 2003.

[9] Wei Ren, Randal W Beard, et al. Consensus seeking in multiagent systems under dynamically changing interaction topologies. *IEEE Transactions on Automatic Control*, 50(5):655–661, 2005.

[10] Reza Olfati-Saber and Richard M Murray. Consensus problems in networks of agents with switching topology and time-delays. *IEEE Transactions on Automatic Control*, 49(9):1520–1533, 2004.

[11] Ming Cao, A Stephen Morse, and Brian DO Anderson. Reaching a consensus in a dynamically changing environment: A graphical approach. *SIAM Journal on Control and Optimization*, 47(2):575–600, 2008.

[12] Yoonsoo Kim and Mehran Mesbahi. On maximizing the second smallest eigenvalue of a state-dependent graph Laplacian. *IEEE transactions on Automatic Control*, 51(1):116–120, 2006.

[13] Andrew Clark, Qiqiang Hou, Linda Bushnell, and Radha Poovendran. Maximizing the smallest eigenvalue of a symmetric matrix: A submodular optimization approach. *Automatica*, 95:446–454, 2018.

[14] Tamás Vicsek and Anna Zafeiris. Collective motion. *Physics Reports*, 517(3):71–140, 2012.

[15] Michele Ballerini, Nicola Cabibbo, Raphael Candelier, Andrea Cavagna, Evaristo Cisbani, Irene Giardina, Vivien Lecomte, Alberto Orlandi, Giorgio Parisi, Andrea Procaccini, et al. Interaction ruling animal collective behavior depends on topological rather than metric distance: Evidence from a field study. *Proceedings of the National Academy of Sciences*, 105(4):1232–1237, 2008.

[16] Haibin Shao, Lulu Pan, Mehran Mesbahi, Yugeng Xi, and Dewei Li. Relative tempo of distributed averaging on networks. *Automatica*, 105:159–166, 2019.

[17] Haibin Shao, Lulu Pan, Mehran Mesbahi, Yugeng Xi, and Dewei Li. Distributed neighbor selection in multi-agent networks. *IEEE Transactions on Automatic Control*, 2023.

[18] Lulu Pan, Haibin Shao, Mehran Mesbahi, Dewei Li, and Yugeng Xi. Structural adaptivity of directed networks. *arXiv preprint arXiv:2208.13223*, 2022.

[19] Wei Ren and Randal W Beard. *Distributed consensus in multi-vehicle cooperative control*, volume 27. Springer, 2008.

[20] Yongcan Cao, Wei Ren, and Magnus Egerstedt. Distributed containment control with multiple stationary or dynamic leaders in fixed and switching directed networks. *Automatica*, 48(8):1586–1597, 2012.

[21] Wenwu Yu, Guanghui Wen, Guanrong Chen, and Jinde Cao. *Distributed cooperative control of multi-agent systems*. John Wiley & Sons, 2017.

[22] Haibin Shao, Mehran Mesbahi, and Yugeng Xi. The relative tempo of discrete-time consensus networks. In *Control Conference (CCC), 2015 34th Chinese*, pages 7362–7367. IEEE, 2015.

[23] Wen Xing, Yuxin Zhao, and Hamid Reza Karimi. Convergence analysis on multi-auv systems with leader-follower architecture. *IEEE Access*, 5:853–868, 2017.